Journal of Molecular and Cellular Cardiology 129 (2019) 208–218

Contents lists available at ScienceDirect

Journal of Molecular and Cellular Cardiology

journal homepage: www.elsevier.com/locate/yjmcc

Original article

Myofilament Ca^{2+} sensitivity correlates with left ventricular contractility during the progression of pressure overload-induced left ventricular myocardial hypertrophy in rats

Mihály Ruppert[a,b,*,1], Beáta Bódi[c,1], Sevil Korkmaz-Icöz[b], Sivakkanan Loganathan[b], Weipeng Jiang[b], Lorenz Lehmann[d], Attila Oláh[a], Bálint András Barta[a], Alex Ali Sayour[a,b], Béla Merkely[a], Matthias Karck[b], Zoltán Papp[c,e], Gábor Szabó[b,1], Tamás Radovits[a,1]

[a] Heart and Vascular Center, Semmelweis University, Budapest, Hungary
[b] Department of Cardiac Surgery, University of Heidelberg, Heidelberg, Germany
[c] Division of Clinical Physiology, Department of Cardiology, Faculty of Medicine, University of Debrecen, Debrecen, Hungary
[d] Department of Cardiology, Angiology and Pulmonology, University Hospital Heidelberg, Heidelberg, Germany
[e] HAS-UD Vascular Biology and Myocardial Pathophysiology Research Group, Hungarian Academy of Sciences, Debrecen, Hungary

ARTICLE INFO

Keywords:
Myocardial hypertrophy
Myofilament function
Ca^{2+} sensitivity
Contractility

ABSTRACT

Aim: Here we aimed at investigating the relation between left ventricular (LV) contractility and myofilament function during the development and progression of pressure overload (PO)-induced LV myocardial hypertrophy (LVH).

Methods: Abdominal aortic banding (AB) was performed to induce PO in rats for 6, 12 and 18 weeks. Sham operated animals served as controls. Structural and molecular alterations were investigated by serial echocardiography, histology, quantitative real-time PCR and western blot. LV function was assessed by pressure-volume analysis. Force measurement was carried out in permeabilized cardiomyocytes.

Results: AB resulted in the development of pathological LVH as indicated by increased heart weight-to-tibial length ratio, LV mass index, cardiomyocyte diameter and fetal gene expression. These alterations were already present at early stage of LVH (AB-week6). Furthermore, at more advanced stages (AB-week12, AB-week18), myocardial fibrosis and chamber dilatation were also observed. From a hemodynamic point of view, the AB-wk6 group was associated with increased LV contractility, maintained ventriculo-arterial coupling (VAC) and preserved systolic function. In the same experimental group, increased myofilament Ca^{2+} sensitivity (pCa_{50}) and hyperphosphorylation of cardiac troponin-I (cTnI) at Threonine-144 was detected. In contrast, in the AB-wk12 and AB-wk18 groups, the initial augmentation of LV contractility, as well as the increased myofilament Ca^{2+} sensitivity and cTnI (Threonine-144) hyperphosphorylation diminished, leading to impaired VAC and reduced systolic performance. Strong correlation was found between LV contractility parameters and myofilament Ca^{2+}-sensitivity among the study groups.

Conclusion: Changes in myofilament Ca^{2+} sensitivity might underlie the alterations in LV contractility during the development and progression of PO-induced LVH.

Abbreviations: AB, aortic banding; ANP, atrial natriuretic peptide; AWT_d, anterior wall thickness in diastole; β/α-MHC, beta/alpha myosin heavy chain ratio; CD, cardiomyocyte diameter; cMyBP-C, cardiac myosin binding protein-C; CO, cardiac output; cTnI, cardiac troponon-I; dP/dt_{max}, maximal slope of systolic pressure increment; dP/dt_{min}, maximal slope of diastolic pressure decrement; dP/dt_{max}-EDV, dP/dt_{max}-end-diastolic volume relationship; E_a, arterial elastance; EDPVR, end-diastolic pressure-volume relationship; ESPVR, end-systolic pressure-volume relationship; F_{max}, Ca^{2+}-saturated maximal force; $F_{passive}$, Ca^{2+}-independent passive tension; HW/TL, heart weight to tibial length ratio; LVEDD, left ventricular end-diastolic diameter; MAP, mean arterial pressure; pCa_{50}, myofilament Ca^{2+} sensitivity; PO, pressure overload; PRSW, preload recruitable stroke work; P–V, pressure–volume; PWT_d, posterior wall thickness in diastole; SV, stroke volume; SW, stroke work; Tau, time constant of left ventricular pressure decay; VAC, ventriculo-arterial coupling

* Corresponding author at: Experimental Research Laboratory, Heart and Vascular Center, Semmelweis University, 1122 Budapest, Városmajor u. 68., Hungary.
E-mail address: ruppertmis@gmail.com (M. Ruppert).

[1] Authors Mihály Ruppert and Beáta Bódi, Gábor Szabó and Tamás Radovits contributed equally to this work.

https://doi.org/10.1016/j.yjmcc.2019.02.017
Received 12 December 2018; Received in revised form 31 January 2019; Accepted 28 February 2019
Available online 04 March 2019
0022-2828/ © 2019 The Authors. Published by Elsevier Ltd. This is an open access article under the CC BY-NC-ND license (http://creativecommons.org/licenses/BY-NC-ND/4.0/).

1. Introduction

During the development of pressure overload (PO)-induced pathological left ventricular (LV) myocardial hypertrophy (LVH) and its progression to heart failure (HF) distinct alterations could be observed in LV contractility. Per definition, the term of contractility defines the intrinsic ability of the myocardium to contract independently of preload and afterload [1]. To date, pressure-volume (P–V) analysis represents the gold standard method to assess the contractile state of the LV in vivo [2]. Therefore, our knowledge regarding the alterations of LV contractility in PO-induced LVH is derived from P–V analysis data. These invasive hemodynamic measurements revealed, that the early stage of LVH is characterized by enhanced LV contractility [3–5]. This contractility augmentation ensures the heart to compensate for the increased PO, thereby maintaining an optimal matching between the contractile state of the LV and the afterload of the connecting arterial system (intact ventriculo-arterial coupling; VAC) [6]. Hence, the early stage of LVH (also referred to as a compensatory stage) is characterized by preserved systolic function. However, in case of PO-induced pathological LVH, the contractility augmentation provides only a temporary adaptation. Consequently, at more advanced stages of LVH the initially enhanced LV contractility declines [5,7]. This leads to an ineffective contra-regulation of the increased arterial afterload (contractility-afterload mismatch) that ultimately manifests in reduced systolic performance.

Recently, it has been suggested that chronic PO induces not only alterations in the contractile state of the LV as an intact organ, but also certain functional changes at the level of the sarcomere. For instance, in animal models with LVH and preserved systolic function, increased myofilament Ca^{2+} sensitivity (pCa_{50}) was observed [8]. In contrast, in rodent models of transverse aortic constriction (TAC)-induced LVH with severely impaired systolic function, reduction in myofilament Ca^{2+} sensitivity and decreased Ca^{2+}-saturated maximal force (F_{max}) was reported [9,10].

Previous results in permeabilized cardiomyocytes along with data of P–V analysis indicate that dynamic alterations might occur in sarcomere function as well (pCa_{50} and/or F_{max}) during the progression of LVH. However, to the best of our knowledge none of the previous studies aimed at investigating isolated, permeabilized cardiomyocyte function in a longitudinal fashion (repetitive measurements in the same experimental model to explore timeline alterations) in case of PO-induced LVH. Furthermore, measurement of LV contractility and myofilament function within one, single experiment has neither been assessed.

Therefore, in the present study we aimed to characterize the alterations in LV contractility as well as sarcomere function at different stages of PO-induced LVH in a relevant rat model.

2. Methods

2.1. Animals

The investigation conformed to the EU Directive 2010/63/EU and the Guide for the Care and Use of Laboratory Animals used by the US National Institutes of Health (NIH Publication No.85–23, revised 1996). The experiments were approved by the ethics committee of the Land Baden-Württemberg for Animal Experimentation (G-94/15). Sprague-Dawley rats (n = 67; 5–6 weeks-old; 160-180 g; Janvier, France) were kept under standard conditions (22 ± 2 °C with 12 h light/dark cycles) and were allowed access to laboratory rat diet and water ad libitum. Furthermore, to eliminate any sex-related differences on the development of PO-induced LVH, only male rats were used in this study.

2.2. Abdominal aortic banding

After a one-week-long acclimatization period, abdominal aortic banding (AB) or sham operation was performed, as also described elsewhere [6]. In brief, under isoflurane anesthesia a midline laparotomy was carried out. Then, the intestinal tract was gently placed aside and the peritoneal layer was dissected in order to gain access to the retroperitoneal space. The abdominal aorta between the right renal artery and the superior mesenteric artery was carefully cleaned from the surrounding connective tissue. A blunted 22-gauge needle was utilized to constrict the aorta above the right renal artery. After AB was completed, the intestines were placed back to the abdominal cavity and the abdominal muscle layer was sutured in single interrupted fashion. Finally, the skin wound was closed by applying surgical clips. Following surgery, analgesia was provided by subcutaneously administered buprenorphine in the dose of 0.05 mg/kg. Sham-operated animals were subjected to the same surgical procedure, except the aortic constriction.

2.3. Experimental groups

Following surgeries, the rats were divided into 6 experimental groups:

Sham-wk6 group (n = 9): after sham operation the rats were followed-up for 6 weeks;

AB-wk6 group (n = 13): after AB the rats were followed-up for 6 weeks;

Sham-wk12 group (n = 9): after sham operation the rats were followed-up for 12 weeks;

AB-wk12 group (n = 13): after AB the rats were followed-up for 12 weeks;

Sham-wk18 group (n = 10): after sham operation the rats were followed-up for 18 weeks;

AB-wk18 group (n = 13): after AB the rats were followed-up for 18 weeks, respectively.

2.4. Echocardiography

Echocardiography was carried out using the Vevo® 2100 imaging system (FujiFilm VisualSonics Inc., Toronto, Ontario, Canada) equipped with a 21-MHz linear probe according to the previously described protocol [6]. Repetitive measurements were performed in the AB-wk18 and Sham-wk18 groups at baseline and 3, 6, 9, 12, 15 and 18 weeks after AB/Sham operation. On M-mode recording images, LV internal diameters (LV end-diastolic diameter [LVEDD] and LV end-systolic diameter [LVESD]) and anterior (AWT) and posterior wall thicknesses (PWT) in diastole (d) and systole (s) were measured and LV mass index (LV mass/body weight) were calculated.

2.5. Pressure–volume analysis

LV P–V analysis was performed according to a previously described protocol with minor modifications [6]. At the end of the experimental period (at week 6, 12 or 18 respectively), rats were anaesthetized by inhalation of 5% isoflurane gas in a chamber. After anesthesia was induced, rats were placed in a supine position on an automatic heating pad to keep the core temperature at 37 °C. To maintain anesthesia during the whole hemodynamic measurement, rats were tracheotomized, intubated, and artificially ventilated with 1–1.5% isoflurane gas in 100% O_2. Pancuronium was administered intraperitoneally (in the dose of 2 mg/kg) to induce muscle relaxation. A polyethylene catheter was inserted into the left external jugular vein for fluid administration. A 2-Fr microtip pressure-conductance catheter (SPR-838, Millar Instruments, Houston, TX) was inserted into the right carotid artery and subsequently advanced into the ascending aorta. After stabilization, arterial blood pressure was recorded. Then the catheter was guided to the LV under pressure control. With the use of a special P–V analysis program (PVAN, Millar Instruments), systolic arterial blood pressure (SBP), diastolic arterial blood pressure (DBP), mean arterial pressure (MAP), maximal slope of systolic pressure increment (dP/dt_{max}) and

Downloaded for Anonymous User (n/a) at HUNGARY - Debrecen University from ClinicalKey.com by Elsevier on March 22, 2019.
For personal use only. No other uses without permission. Copyright ©2019. Elsevier Inc. All rights reserved.

diastolic pressure decrement (dP/dt_{min}), LV end-systolic volume (LVESV), LV end-diastolic volume (LVEDV), stroke volume (SV), ejection fraction (EF), heart rate (HR), cardiac output (CO), stroke work (SW) were computed and calculated. Furthermore, the integrative index of arterial afterload, arterial elastance [E_a; calculated by the following equation: E_a = LVESP/SV [11]], and the time constant of LV pressure decay [Tau; according to the Glanz method [12]] were also assessed.

To detect load-independent contractility parameters, P−V loops were also registered at transiently decreasing preload, which was achieved by transient occlusion of the inferior caval vein. By this maneuver, the following load-independent contractility indexes were calculated: the slope of the end-systolic P−V relationship (ESPVR, according to the parabolic curvilinear model [13]), preload recruitable stroke work (PRSW) and the slope of the dP/dt_{max}-end-diastolic volume relationship (dP/dt_{max}-EDV).

To characterize myocardial stiffness, the slope of the end-diastolic P−V relationship (EDPVR) was derived.

To assess LV net performance, ventriculo-arterial coupling (VAC) was determined as the ratio of E_a and ESPVR (VAC = E_a/ESPVR) [14].

Parallel conductance was calculated, and volume calibration of the conductance system was performed as previously described [2]. After completion of the hemodynamic measurements, animals were euthanized by exsanguination. After exsanguination, the organs were perfused in situ with cold (4 °C), oxygenated Ringer solution to eliminate erythrocytes from myocardial tissue. Then, heart weights and tibial lengths were quickly measured. The ratio of heart weight-to-tibial length was calculated to assess the extent of LVH.

2.6. Measurement of permeabilized cardiomyocyte mechanical parameters

In each experimental groups, deep-frozen heart tissue samples from 6 animals were used for cardiomyocyte measurements (N = 6). In each groups, a total of 10–12 cardiomyocytes were measured (n = 10–12). Samples were mechanically isolated in isolating solution [(Iso contained: KCl (100 mM), EGTA (2 mM), MgCl2 (1 mM), Na_2ATP (4 mM), imidazole (10 mM), pH = 7.0) containing phenylmethylsulfonyl fluoride (PMSF, 0.5 mM, Sigma–Aldrich, St. Louis, MO, USA), leupeptin (40 μM, Sigma–Aldrich), and E-64 (10 μM, Sigma–Aldrich) protease inhibitors at 4 °C. Cardiomyocytes were permeabilized with 0.5% Triton X-100 detergent for 4 min to remove all membranous structures. Single isolated and permeabilized cardiomyocytes were mounted between two thin stainless insect needles by means of silicone adhesive (DAP 100% all-purpose silicone sealant; Baltimore, MD, USA) at 15 °C. The needles were connected to a highly sensitive force transducer (SensoNor, Horten, Norway) and an electromagnetic length controller (Aurora Scientific Inc., Aurora, Canada). Activating and relaxing solutions were mainly used during the force measurement procedure. The activating solution contained: CaEGTA (7 mM), KCl (37.34 mM), N,N-bis (2-hydroxyethyl)-2-aminoethanesulfonic acid (BES, 10 mM), $MgCl_2$ (6.24 mM), Na_2ATP (6.99 mM), Na_2CrP (15 mM), pH = 7.2 resulting in a $[Ca^{2+}]$ of pCa = 4.75 (pCa: -lg$[Ca^{2+}]$). The relaxing solution contained the same components apart from containing EGTA instead of CaEGTA, pH = 7.2 resulting in a $[Ca^{2+}]$ of pCa = 9. Both solutions were supplemented with protease inhibitors. Solutions with intermediate calcium concentrations were prepared by mixing relaxing and activating solutions (pCa 5.4–7.0). The sarcomere length (SL) was adjusted to 2.3 μm. The active force (F_{active}) and Ca^{2+}-sensitivity of force production were determined in activating solutions with different Ca^{2+} concentrations. When the maximal active force (F_{max}) had been reached, a quick release-restretch maneuver (30 ms) was applied in the activating solution. The length of the myocyte was reduced by 20% followed by quick re-stretching the cell back to its initial length (release–restretch maneuver).

The Ca^{2+}-independent passive tension ($F_{passive}$) was approximated by shortening of the preparations to 80% of the original lengths in relaxing solution for 8 s. The cell was then exposed to a series of solutions containing intermediate pCa to construct the pCa-force relationship. F_{active} at submaximal Ca^{2+} levels were normalized to the F_{active} at maximal Ca^{2+} level (4.75, F_{max}). The relation between the F_{active} and pCa was fitted to a modified Hill equation: $F_{total} = F_{max}[Ca^{2+}]^{nHill}/(pCa_{50}{}^{nHill} + [Ca^{2+}]^{nHill}) + F_{passive}$, where F_{max} is the maximal force, $F_{passive}$ is the passive force, $F_{total} = F_{max} + F_{passive}$, $[Ca^{2+}]$ is the calculated Ca^{2+} concentration, nHill is a constant the slope and the midpoint of the sigmoidal relationship, respectively. pCa_{50} illustrated the Ca^{2+} concentration at which half of the maximal force was produced. The values of absolute forces were normalized to myocyte cross sectional area and expressed in kN/m^2.

Ca^{2+}-induced contractures of cardiomyocytes were recorded by a custom-built LABVIEW Data Acquisition platform and analyzed by LabVIEW analysing software (Myo; National Instruments, Austin, TX, USA).

2.7. Western immunoblotting

Cardiomyocytes were isolated and permeabilized from frozen LV heart tissues, then myocytes were solubilized in sample buffer (containing 8 M urea, 2 M thiourea, 3% (*w/v*) sodium dodecyl sulfate (SDS), 75 mM DTT, 50 mM Tris-HCl, pH 6.8, 10% (*v/v*) glycerol, 0.5% bromophenol blue, 40 μM leupeptin and 10 μM E-64) for 45 min vortexing. After centrifugation (16,000 *g* for 5 min at 24 °C), protein amount of supernatant was determined by dot-blot technique using bovine serum albumin (BSA) standard, and the concentration of samples were set to 2 mg/ml. Cardiac troponin-I (cTnI) and myosin binding protein-C (cMyBP-C) were carried out with 12% and 4% gradient gels. Western immunoblotting was applied to assess the site-specific phosphorylation status of cardiac proteins. After protein blotting, the membranes were blocked with 2% BSA diluted in PBS containing 0.1% (*v/v*) Tween 20 (PBST) for 30 min, then cTnI phosphorylation-sensitive antibodies were used to determine the levels of protein kinase A (PKA) and protein kinase C (PKC)-dependent cTnI (Ser-23/24 (1:1000), Ser-43 (1:500) and Thr-144 (1:500), Abcam, Cambridge, UK) and PKA-dependent cMyBP-C (Ser-282 (1:500, Enzo Life Sciences, Farmingdale, New York) phosphorylation. The signal was detected with a peroxidase-conjugated anti-rabbit IgG secondary antibody (1:300) (Sigma–Aldrich, St.Louis, MO, USA) on the membranes. Total amount of cTnI was visualized with super sensitive membrane staining (UD-GenoMed, Debrecen, Hungary). Chemiluminescence (ECL) signals were normalized to western blot stain.

2.8. Histology

The hearts were fixed in buffered paraformaldehyde solution (4%) and embedded in paraffin. Transverse, transmural, 5-μm thick slices of the ventricles were cut and placed on adhesive slides.

Hematoxylin and eosin staining was performed to define cardiomyocyte diameter (CD) as a cellular marker of myocardial hypertrophy [15]. In each sample, 100 longitudinally oriented cardiomyocytes from the LV were examined, and the diameters at transnuclear position were measured. The mean value of 100 measurements represented 1 sample.

The extent of myocardial fibrosis was assessed on picrosirius-stained sections [16]. ImageJ software (NIH, Bethesda, MD) was used to identify the picrosirius red-positive area. Three transmural images were randomly taken from the LV wall on each section. After background subtraction, eye-controlled auto-threshold has been determined to detect positive areas. The collagen area (picrosirius red-positive area – to - total area ratio) was determined on each image, and the mean value of three images represents each animal.

2.9. LV mRNA expression analysis

LV mRNA analysis was performed according to the previously

Downloaded for Anonymous User (n/a) at HUNGARY - Debrecen University from ClinicalKey.com by Elsevier on March 22, 2019.
For personal use only. No other uses without permission. Copyright ©2019. Elsevier Inc. All rights reserved.

described protocol [7]. Briefly, LV myocardium was homogenized in a lysis buffer (RLT buffer; Qiagen, Hilden, Germany). RNA was isolated using the RNeasy Fibrous Tissue Mini Kit (Qiagen), according to the manufacturer's instructions. The quality and concentration of the isolated RNA were assessed by the NanoDrop 2000 Spectrophotometer (Thermo Scientific™, Waltham, MA, USA). Accordingly, optical density at 230, 260, and 280 nm was measured. The ratios of 230/260 and 230/280 nm were defined for quality control. Reverse transcription reaction (1 μg total RNA of each sample) was completed using the QuantiTect Reverse Transcription Kit (Qiagen). Quantitative real-time PCR was performed with the StepOnePlus Real-Time PCR System (Applied Biosystems, Foster City, CA, USA) in duplicates of each sample in a volume of 10 μl in each well containing cDNA (1 μl), TaqMan Universal PCR MasterMix (5 μl), and a TaqMan Gene Expression Assay (0.5 μl) (Applied Biosystems) for the following genes: atrial natriuretic peptid (ANP; assay ID: Rn00664637_g1), β-type myosin heavy chain (β-MHC; assay ID: Rn00568328_m1), α-type myosin heavy chain (α-MHC; assay ID: Rn00568304_m1). Gene expression data were normalized to glyceraldehyde 3-phosphate dehydrogenase (GAPDH; assay ID: Rn01775763_g1), and expression levels were calculated using the CT comparative method ($2^{-\Delta CT}$). All results are expressed as values normalized to a positive calibrator (a pool of cDNA from all samples of the Sham-wk6 group [$2^{-\Delta\Delta CT}$]).

2.10. Statistics

All values are expressed as mean ± standard error of the mean. The distribution of the datasets was tested by D'Agostino-Pearson omnibus and Shapiro-Wilk normality test.

An unpaired two-sided Student's *t*-test in case of normal distribution or Mann-Whitney *U* test in case of non-normal distribution was used to compare two independent groups.

Two-way analysis of variance (ANOVA) with the factors "time" and "aortic banding" were carried out to compare six independent groups. For values of P_{time}, $P_{aortic\ banding}$ and $P_{interaction}$ see Suppl. Table 1. Prior to two-way ANOVA, those datasets that failed to show normal distribution were logarithmically transformed. Tukey post hoc test was utilized to detect intergroup differences.

Repeated-measures one-way ANOVA or Friedman test was performed for comparing data of the echocardiographic measurements at different time points (week 3, 6, 9, 12, 15 and 18) within a group. To examine intergroup differences, Holm-Sidak or Dunn post hoc test was carried out.

According to the distribution of the datasets, Pearson (in case of normal) or Spearman (in case of not-normal) correlation test was performed to detect correlations between pCa_{50} and ESPVR, between pCa_{50} and PRSW and between pCa_{50} and dP/dt_{max}-EDV.

Western immunoblot assays were performed in triplicate. Intensities of protein bands were quantified by determining the area under the intensity curves by a Gaussian fit using ImageJ (National Institutes of Health, Bethesda, MD, USA) and Magic Plot (Saint Petersburg, Russia) software.

A *P* value of < 0.05 was used as a criterion for statistical difference. Furthermore, two additional categories ($P < .01$ and $P < .001$) were introduced to indicate the strength of the observed statistical difference.

2.11. Data availability

The raw data from the current study will be made available by the corresponding author upon reasonable request.

Table 1
LV and myofilament function in aortic-banded and sham-operated rats at different time points.

	Week 6		Week 12		Week 18	
	Sham (n = 9)	*AB* (n = 13)	*Sham* (n = 9)	*AB* (n = 13)	*Sham* (n = 10)	*AB* (n = 13)
SBP, mmHg	148 ± 4	215 ± 4***	138 ± 5	215 ± 5***	150 ± 5	228 ± 4***
DBP, mmHg	116 ± 3	150 ± 2***	110 ± 4	154 ± 4***	120 ± 4	170 ± 3***###$$
MAP, mmHg	127 ± 4	172 ± 2***	119 ± 4	174 ± 4***	140 ± 4	189 ± 3***##$
E_a, mmHg/μl	0.75 ± 0.06	1.20 ± 0.08*	0.68 ± 0.05	1.33 ± 0.10***	0.84 ± 0.05	1.54 ± 0.16***
HR, beats/min	355 ± 7	369 ± 9	354 ± 5	366 ± 7	379 ± 7	357 ± 5
dP/dt_{max}, mmHg/s	8018 ± 314	10,781 ± 283***	8425 ± 365	10,692 ± 374**	9689 ± 322	10,810 ± 518
dP/dt_{min}, mmHg/s	−8587 ± 221	−10,663 ± 343**	−9277 ± 344	−9681 ± 249	−10,073 ± 331	−9000 ± 431##
LVEDV, μl	268 ± 16	305 ± 14	286 ± 23	320 ± 20	283 ± 18	327 ± 14
LVESV, μl	175 ± 15	194 ± 12	178 ± 17	231 ± 11	160 ± 11	241 ± 11***
SV, μl	188 ± 16	173 ± 10	195 ± 11	163 ± 12	175 ± 10	151 ± 15
CO, ml/min	66.7 ± 6.1	62.9 ± 3.0	69.4 ± 4.5	59.4 ± 4.1	66.3 ± 4.4	53.7 ± 5.4
SW, mmHg*μl	17,314 ± 1300	25,194 ± 1873	18,404 ± 988	22,005 ± 2677	17,674 ± 1296	20,405 ± 1855
EF, %	58 ± 3	51 ± 2	57 ± 2	44 ± 2**	55 ± 2	41 ± 3***##
Tau, ms	14.2 ± 0.4	18.4 ± 0.9**	12.8 ± 0.6	19.4 ± 0. 6***	13.0 ± 0.3	21.7 ± 1.2***#
EDPVR, mmHg/μl	0.038 ± 0.005	0.038 ± 0.007	0.028 ± 0.004	0.042 ± 0.006	0.014 ± 0.003	0.032 ± 0.004**
VAC	0.50 ± 0.08	0.45 ± 0.06	0.54 ± 0.06	0.76 ± 0.08##	0.57 ± 0.10	0.87 ± 0.08###
F_{max}, kN/m^2	15.3 ± 0.8	13.6 ± 0.7	14.2 ± 0.5	13.1 ± 0.8	13.6 ± 0.8	15.5 ± 1.0

Values are expressed as mean ± standard error of the mean. AB indicates aortic-banding; SBP: systolic arterial blood pressure; DBP: diastolic arterial blood pressure; MAP: mean arterial pressure; E_a: arterial elastance, HR: heart rate; dP/dt_{max}: maximal slope of systolic pressure increment; $dP/dt_{min:}$ maximal slope of diastolic pressure decrement; LVEDV: LV end-diastolic volume; LVESV: LV end-systolic volume; SV: stroke volume; CO: cardiac output; SW: stroke work; EF: ejection fraction; Tau: time constant of LV pressure decay according to the Glantz' method; EDPVR: end-diastolic pressure-volume relationship; VAC: ventriculo-arterial coupling; F_{max}: Ca^{2+}-saturated maximal force. *: $P < .05$ vs. age-matched sham.

** $P < .01$ vs. age-matched sham.

*** $P < .001$ vs. age-matched sham.

# $P < .05$ vs. AB-week 6.

$P < .01$ vs. AB-week 6.

$P < .001$ AB-week 6.

$ $P < .05$ vs. AB-week 12.

$$ $P < .01$ vs. AB-week 12.

Downloaded for Anonymous User (n/a) at HUNGARY - Debrecen University from ClinicalKey.com by Elsevier on March 22, 2019.
For personal use only. No other uses without permission. Copyright ©2019. Elsevier Inc. All rights reserved.

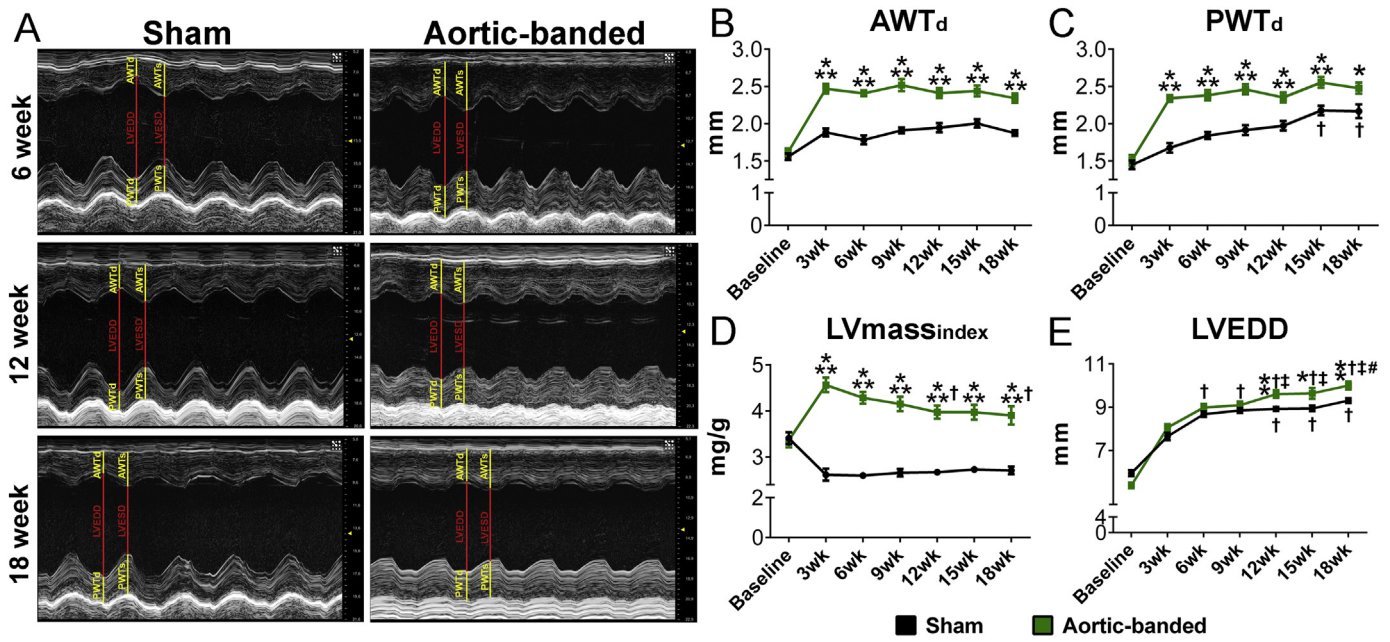

Fig. 1. Echocardiographic follow-up during the development of pressure overload-induced LVH.
Representative M-mode echocardiographic images at the midpapillary muscle level are shown at week 6, 12 and 18 (A). The temporal development of pressure overload-induced left ventricular (LV) myocardial hypertrophy in the aortic-banded (AB) group (AB-wk18 group) was associated with increased anterior wall thickness in diastole (AWT_d) (B), increased posterior wall thickness in diastole (PWT_d) (C) and increased LV mass index (D) compared to the corresponding sham group (sham-wk18 group). Furthermore, from week 12 to week 18, increment in LV end-diastolic diameter revealed chamber dilatation in the AB-wk18 group. *: $P < .05$ vs. corresponding sham. **: $P < .01$ vs. corresponding sham. ***: $P < .001$ vs. corresponding sham. †: $P < .05$ vs. week 3. ‡: $P < .05$ vs. week 6. #: $P < .05$ vs. week 9.

3. Results

3.1. Echocardiographic follow-up during the development of PO-induced LVH

From week 3 until the end of the experimental period, AWT_d, PWT_d and $LVmass_{index}$ were increased in the AB-wk18 group compared to the sham-wk18 group, indicating the development of LVH (Fig. 1B-D). Furthermore, at week 12, week 15 and week 18, LVEDD was also increased in the AB-wk18 group compared to the sham-wk18 group, suggesting chamber dilatation (Fig. 1E).

3.2. Pathological hypertrophy and fibrosis markers in PO-induced LVH

In the AB-wk6, AB-wk12 and AB-wk18 groups, HW/TL and CD were increased compared to the corresponding sham groups (Fig. 2B–C). The myocardial mRNA expression levels of β/α-MHC ratio and ANP were also elevated in the AB groups compared to their corresponding sham groups, indicating reactivation of the fetal gene program (Fig. 2D–E). Furthermore, assessment of the myocardial collagen area revealed increased interstitial fibrosis in the AB-wk12 and AB-wk18 groups compared to the sham-wk12 and sham-wk18 groups, respectively (Fig. 2F).

3.3. Myofilament function

pCa_{50} increased significantly in the AB-wk6 group compared to the sham-wk6 group, indicating increased myofilament Ca^{2+} sensitivity (Fig. 3). This pCa_{50} value was also significantly higher in the AB-wk6 group than in the AB-wk12 and AB-wk18 groups (Fig. 3). Myofilament Ca^{2+} sensitivity in the AB-wk12 and AB-wk18 groups did not differ from their corresponding sham groups (Fig. 3).

Furthermore, no significant differences could be observed in F_{max} among the experimental groups (Table 1).

3.4. Site-specific phosphorylation of cardiac troponin-I and myosin binding protein-C

Phosphorylation of cTnI at Ser-22/23 and Ser-43 did not differ among the study groups (Fig. 4A–B). There was also no difference in the phosphorylation status of cMyBP-C at Ser-282 (Fig. 4D). In contrast, phosphorylation of cTnI at the PKC-specific Thr-144 site was significantly increased in the AB-wk6 group compared either to the sham-wk6 group or the AB-wk12 and AB-wk18 groups (Fig. 4C).

3.5. LV function

Hemodynamic results obtained from P—V analysis are summarized in Figs. 5–7 and Table 1.

3.5.1. Arterial loading

SBP, DBP, MAP and Ea were elevated in the AB groups compared to the corresponding sham groups, confirming the presence of increased PO proximal to the aortic constriction (Table 1).

3.5.2. Load-dependent systolic parameters

The AB-wk6 group was associated with preserved systolic performance. Accordingly, no difference could be observed in load-dependent systolic parameters (EF, SV, CO) between the AB and the sham group at week 6 (Table 1). In contrast, in the AB-wk12 and AB-wk18 groups, EF decreased significantly, while SV and CO showed a tendency towards decreased values compared to the corresponding sham groups (Table 1).

3.5.3. Load-independent contractility parameters

In the AB-wk6 group, ESPVR, PRSW and dP/dt_{max}-EDV increased significantly compared to the sham-wk6 group, indicating increased LV contractility (Figs. 5A–B, 6A–B, 7A–B). This contractility augmentation diminished in the AB-wk12 and AB-wk18 groups. Accordingly, the load-independent contractility parameters were not different in the AB-

Downloaded for Anonymous User (n/a) at HUNGARY - Debrecen University from ClinicalKey.com by Elsevier on March 22, 2019.
For personal use only. No other uses without permission. Copyright ©2019. Elsevier Inc. All rights reserved.

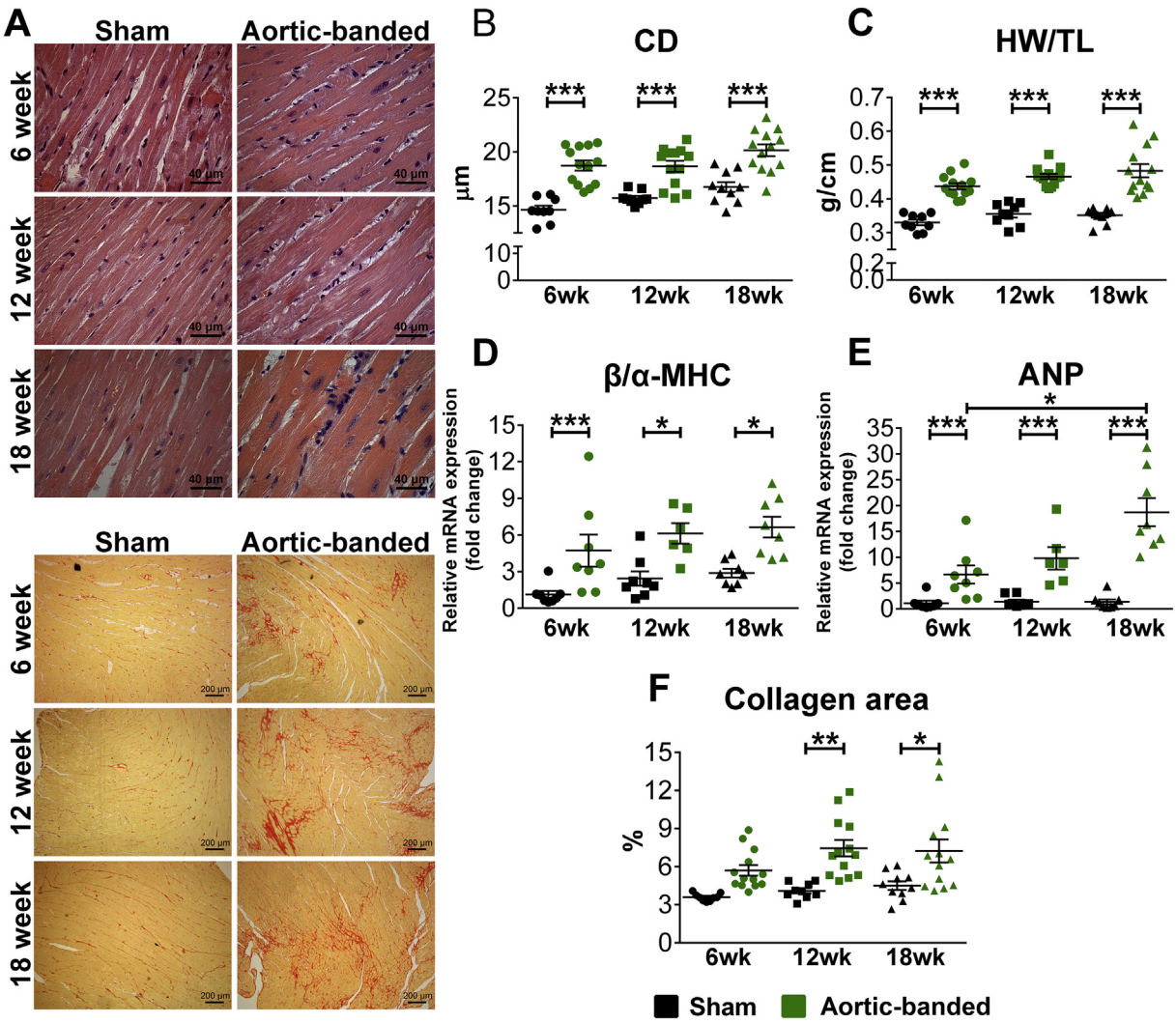

Fig. 2. Pathological hypertrophy markers at different stages of pressure overload-induced LVH.
Representative photomicrographs of hematoxylin and eosin (magnification 200×, scale bar: 40 µm) and picrosirius red staining (magnification 50×, scale bar: 200 µm) are shown demonstrating enlargement of cardiomyocytes and insterstitital collagen accumulation in the aortic-banded (AB) groups (A). The development of pressure overload-induced left ventricular myocardial hypertrophy (LVH) was confirmed by increased heart weight-to-tibial length ratio (HW/TL) (B) and cardiomyocyte diameter (CD) (C) in the AB groups at week 6, 12 and 18 compared to the corresponding sham groups. The pathological nature of LVH was reflected by markers of the fetal gene program (beta-to-alpha myosin heavy chain ratio [β/α-MHC] and atrial natriuretic peptide [ANP]) (D-E). Furthermore, in the AB groups at week 12 and 18, the extent of collagen area increased significantly compared to the corresponding sham groups. *: $P < .05$. **: $P < .01$. ***: $P < .001$. (For interpretation of the references to colour in this figure legend, the reader is referred to the web version of this article.)

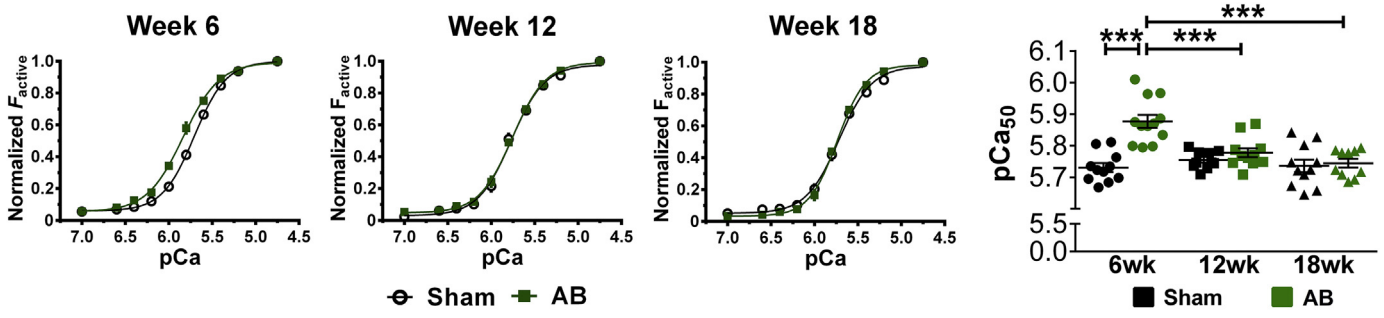

Fig. 3. Myofilament Ca^{2+} sensitivity in pressure overload-induced LVH.
pCa-force relationship of permeabilized cardiomyocytes revealed increased myofilament Ca^{2+}-sensitivity (pCa_{50}) in the aortic-banded (AB) group at week 6 compared to the corresponding sham group and also to the AB groups at week 12 and 18. Experimental values are derived from 6 animals ($N = 6$) and 10–12 cardiomyocytes ($n = 10–12$) per group. ***: $P < .001$.

Downloaded for Anonymous User (n/a) at HUNGARY - Debrecen University from ClinicalKey.com by Elsevier on March 22, 2019.
For personal use only. No other uses without permission. Copyright ©2019. Elsevier Inc. All rights reserved.

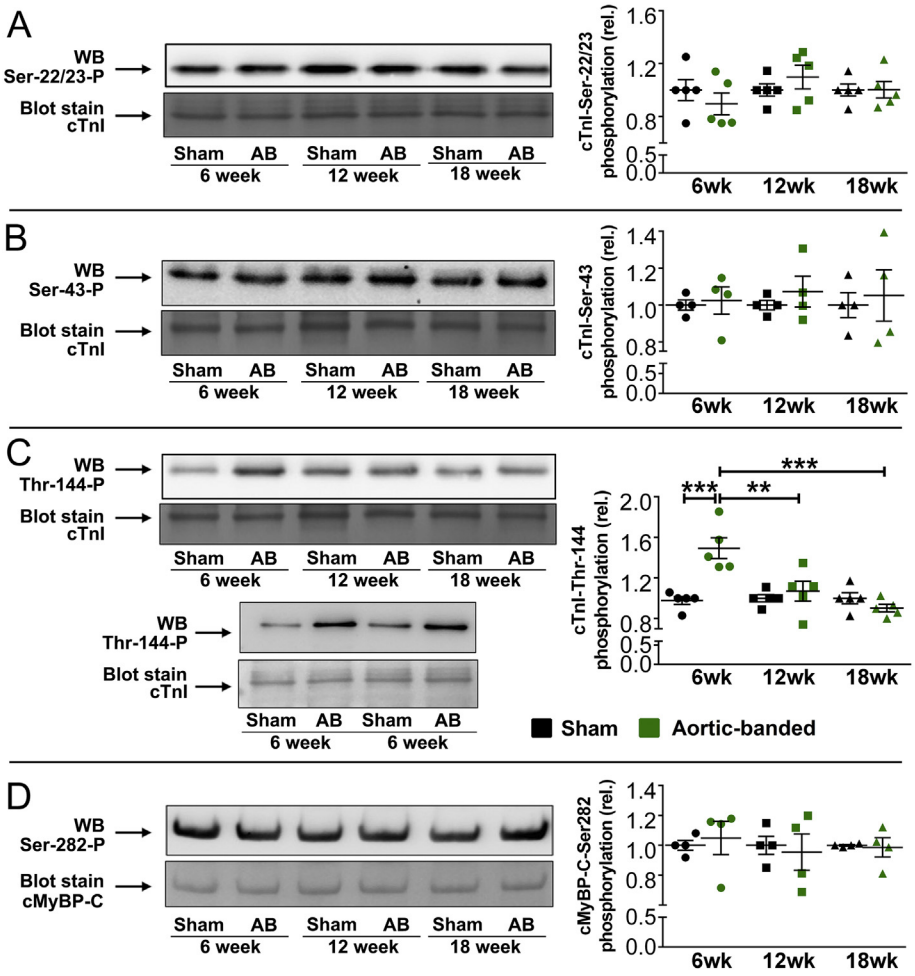

Fig. 4. Site-specific phosphorylation of cardiac troponin-I and myosin binding protein-C.
Western blot analysis revealed unaltered phosphorylation of cTnI at Ser-22/23 (4A) and Ser-43 (4B) and cMyBP-C at Ser-282 (4D) among the study groups. In contrast, phosphorylation of cTnI at Thr-144 increased significantly in the AB-wk6 group compared to the corresponding sham group and also the AB-wk12 and AB-wk18 groups (4C). **: $P < .01$. ***: $P < .001$.

wk12 and AB-wk18 groups compared to sham-wk12 and sham-wk18 groups, but they were significantly decreased compared to the AB-wk6 group (Figs. 5A–B, 6A–B).

3.5.4. Ventriculo-arterial coupling

In the AB-wk6 group, the enhanced LV contractility (increased ESPVR) counterbalanced the elevated afterload (increased E_a), therefore VAC did not differ from the corresponding sham group (Table 1). In contrast, in the AB-wk12 and AB-wk18 groups, the lack of compensatory LV contractility augmentation (reduced ESPVR values compared to AB-wk6) along with the elevated afterload (increased E_a) resulted in contractility-afterload mismatch. Thus, the values of VAC were significantly higher in the AB-wk12 and AB-wk18 groups compared to that of the AB-wk6 group (Table 1).

3.5.5. Diastolic function

Tau increased significantly in the AB-wk6, AB-wk12 and AB-wk18 groups compared to their corresponding sham groups (Table 1). Furthermore, the slope of EDPVR was also elevated in the AB-wk18 group compared to the sham-wk18 group (Table 1).

3.6. Correlation between myofilament Ca^{2+} sensitivity and LV contractility parameters

Strong correlations were detected between the load-independent LV contractility parameters (ESPVR, PRSW and dP/dt_{max}-EDV) and myofilament Ca^{2+} sensitivity (pCa_{50}) (Figs. 5–7).

4. Discussion

The present paper is the first that demonstrates a strong correlation between myofilament Ca^{2+} sensitivity of permeabilized cardiomyocytes (pCa_{50}) and P—V analysis derived LV contractility parameters (ESPVR, PRSW, dP/dt_{max}-EDV) in a rat model of PO-induced LVH. Our results indicate that changes in myofilament Ca^{2+} sensitivity might underlie the alterations in LV contractility during the development and progression of PO-induced LVH.

4.1. Structural and molecular characterization of AB-induced LVH

In the current study the abdominal AB rat model was used to investigate PO-induced remodeling of the LV. Consistently with our previous experiences with this model [4,6,7,16], AB evoked the development of marked LVH, as indicated by echocardiographic data (increased wall thicknesses and $LVmass_{index}$) (Fig. 1B–D), post mortem measurement (increased HW/TL) and histological analysis (increased CD) (Fig. 2A–C). The pathological nature of LVH was confirmed by the reactivation of the fetal gene program (enhanced β/α-MHC ratio and ANP mRNA levels) (Fig. 2D–E) [17]. All of these structural and molecular alterations were already present after 6 weeks of AB. In addition,

Downloaded for Anonymous User (n/a) at HUNGARY - Debrecen University from ClinicalKey.com by Elsevier on March 22, 2019.
For personal use only. No other uses without permission. Copyright ©2019. Elsevier Inc. All rights reserved.

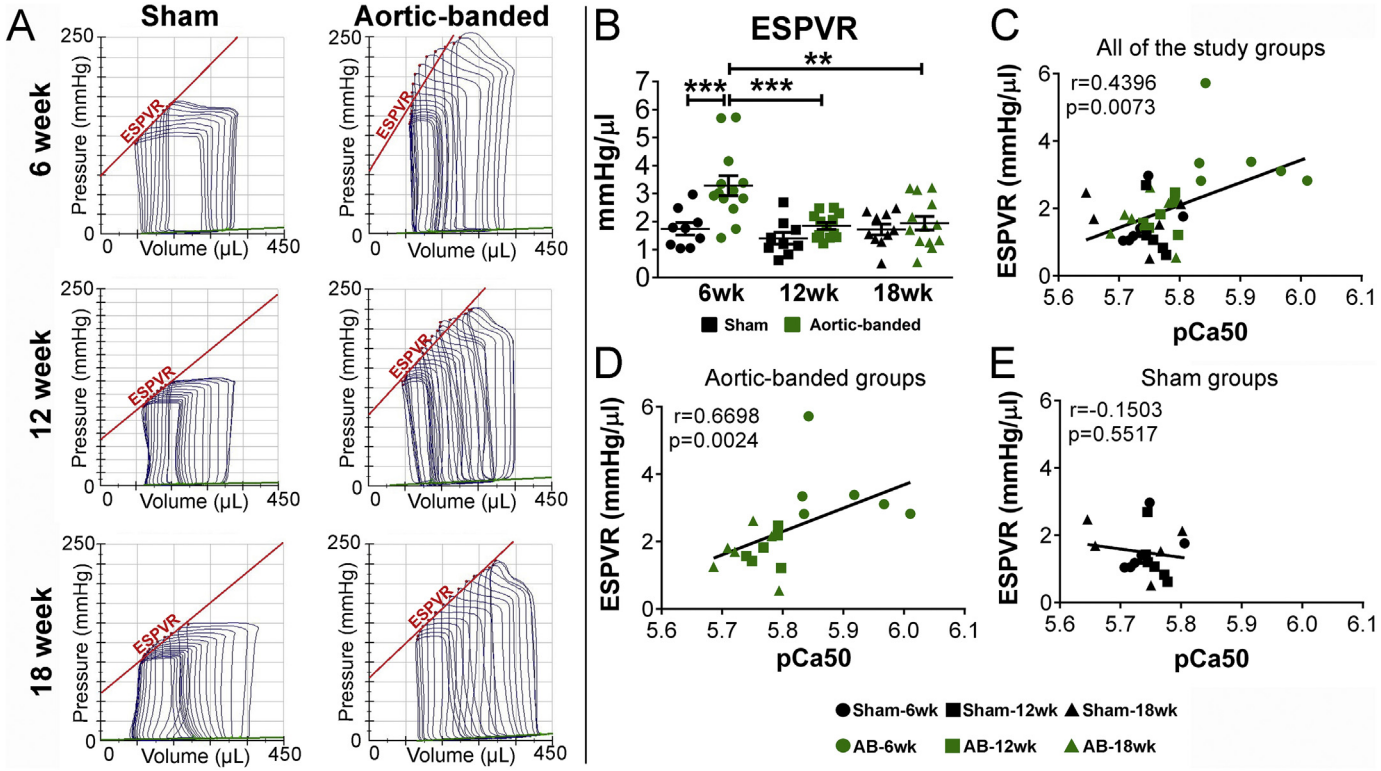

Fig. 5. Correlation between the slope of the end-systolic pressure-volume relationship and myofilament Ca^{2+} sensitivity during the progression of PO-induced LVH. Assessment of the slope of the end-systolic pressure-volume relationship (ESPVR) revealed increased left ventricular (LV) contractility in the aortic-banded (AB) group at week 6 compared to the corresponding sham group and also to the AB groups at week 12 and 18 (A-B). Alterations in ESPVR and pCa_{50} showed a strong correlation among all the study groups (C) and also among only the AB groups (D). No correlation could be detected among the Sham groups (E). LVH indicates left ventricular hypertrophy; PO: pressure overload. **: $P < .01$. ***: $P < .001$.

at later time points (week 12 and week 18) AB was also associated with chamber dilatation and progressive accumulation of interstitial collagen content (Fig. 1E, Fig. 2F), which is also in good agreement with prior findings [18].

4.2. Longitudinal assessment of LV function in PO-induced LVH by P–V analysis

Currently, P–V analysis represents the gold standard method to reliably measure in vivo LV hemodynamics [2]. Of particular interest, the assessment of the P–V loops at different preloads enables us to calculate LV contractility parameters, independently of loading conditions. Therefore, this technique is extremely valuable in pathological states, where the robust alterations in pre- and/or afterload (e.g. AB-induced chronic PO) make the conventional load-dependent parameters inappropriate to characterize LV function. For these reasons, P–V analysis was utilized in the present investigation as well, to explore timeline alterations in LV hemodynamics at different stages of PO-induced LVH.

Early stage of PO-induced LVH. The early stage of PO-induced LVH is typically associated with impaired diastolic function (predominantly prolonged active relaxation) [19], and preserved systolic performance. Although, at this stage, the conventional load-dependent systolic indexes show no alteration, assessment of P–V analysis-derived, load-independent indexes revealed robust augmentation of LV contractility [4,6,16]. This increment in LV contractility allows the LV to compensate for the increased afterload, thereby maintaining an optimal interaction between the LV and the arterial system. Based on our previous experiences with the abdominal AB model [4,16], week 6 was chosen as a time point to investigate the early stage of LVH. According to our expectations, in the AB group at this time point diastolic dysfunction was already present (indicated by prolonged Tau), but the load-dependent systolic indexes (e.g. EF) were preserved (Table 1). To characterize LV contractility independently from extrinsic conditions, three load-independent, gold standard parameters (ESPVR, PRSW and dP/dt_{max}-EDV) were calculated from P–V analysis data [2]. All of these indexes confirmed augmented LV contractility in the AB group (Figs. 4B, 5B, 6B). Furthermore, assessment of VAC ratio confirmed an adequate matching between LV contractility and the afterload of the connecting arterial system (Table 1). Therefore, from a hemodynamic point of view, the AB group at week 6 met the criteria of an early stage of PO-induced LVH.

Advanced stages of PO-induced LVH. In case of PO-induced pathological LVH, the contractility augmentation provides only temporary adaptation. Accordingly, after a certain period of time, the initially increased LV contractility regresses, despite of the persistently elevated PO [5,6]. In animal models of chronic PO-induced LVH, the time point when LV systolic dysfunction is expected to develop is dependent on the species of the experimental animal (mice versus rat), the location of the banding suture (thorax versus abdomen) and the severity of the applied constriction (severe versus moderate) [20]. Our experience from previous consecutive studies with the abdominal AB rat model indicates, that an early transition from “compensated” LVH to systolic dysfunction takes place after 12 weeks of chronic PO in male AB rats [6]. Thus, in the current study, week 12 and week 18 were selected to study advanced stages of LVH. At these time points, the P–V analysis derived contractility indexes were substantially reduced compared to that of the early stage of LVH (AB-wk6 group) (Fig. 4B, 5B, 6B). The decompensation of the hypercontractile state along with increased arterial loading condition (E_a) resulted in contractility-afterload mismatch (impaired VAC ratio) (Table 1). Therefore, at these time points the net systolic performance was decreased, which was reflected by a slight reduction in load-dependent systolic parameters (e.g. EF) (Table 1). Furthermore, the AB-wk18 group was also associated with marked

Downloaded for Anonymous User (n/a) at HUNGARY - Debrecen University from ClinicalKey.com by Elsevier on March 22, 2019.
For personal use only. No other uses without permission. Copyright ©2019. Elsevier Inc. All rights reserved.

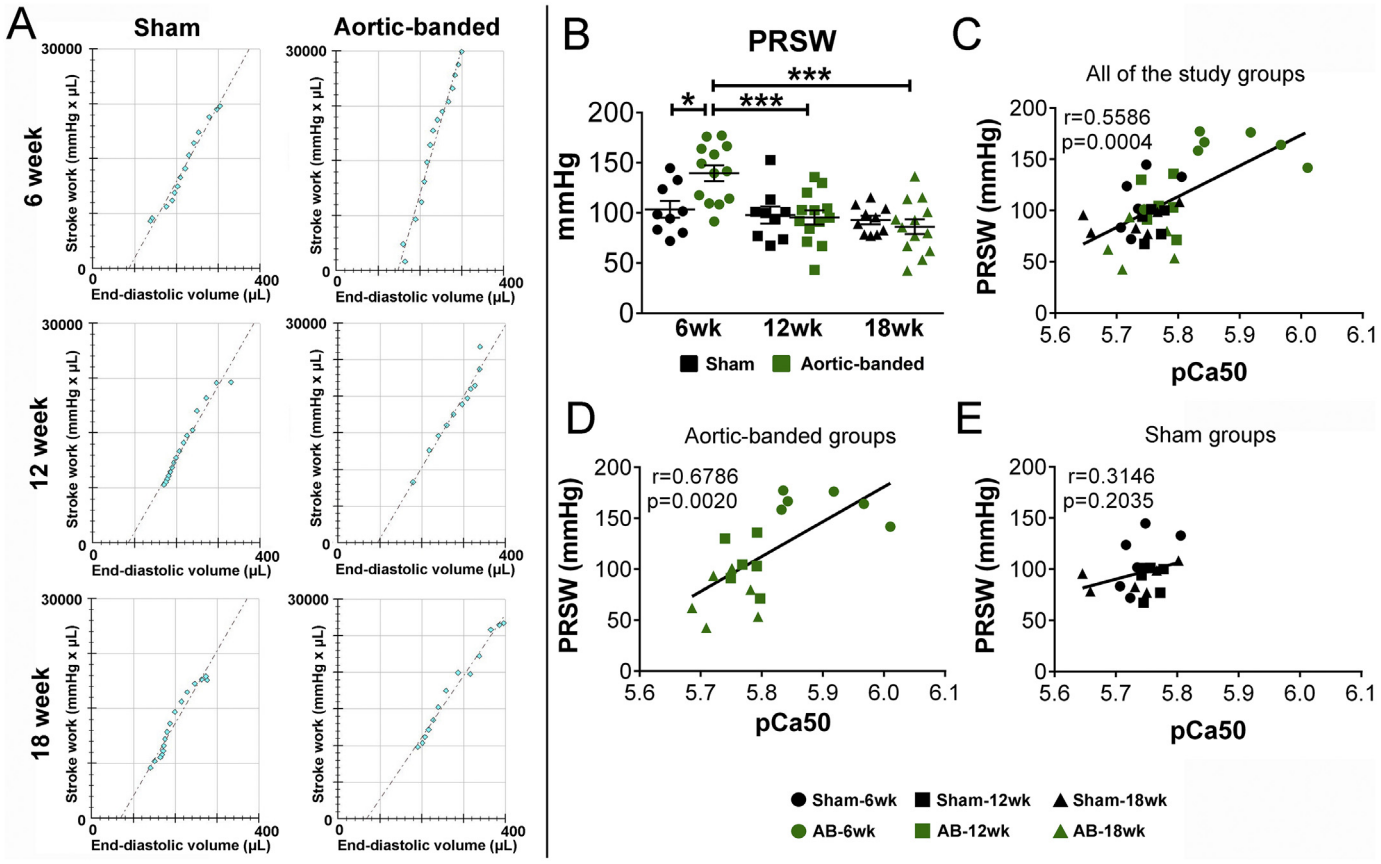

Fig. 6. Alterations in preload recruitable stroke work showed strong correlation with changes in myofilament Ca^{2+} sensitivity during the progression of PO-induced LVH.

Preload recruitable stroke work (PRSW) indicated increased left ventricular (LV) contractility in the aortic-banded (AB) group at week 6 compared to the corresponding sham group and also to the AB groups at week 12 and 18 (A-B). Strong correlation could be observed between PRSW and pCa_{50} among all the study groups (C) and also among only the AB groups (D). No correlation could be detected among the Sham groups (E). LVH indicates left ventricular hypertrophy; PO: pressure overload. *: $P < .05$. ***: $P < .001$.

impairment of both aspects (active relaxation and passive stiffness) of diastolic function (Table 1).

4.3. Myofilament function in PO-induced LVH and its correlation to global LV function

The force generation of cardiomyocytes is eventually dependent on sarcomere function [21]. Therefore, it is reasonable to hypothesize that certain alteration might occur in myofilament function during the development and progression of PO-induced LVH that underlie the observed changes in LV contractility. This is further supported by the fact that former studies reported increased, unaltered and decreased cardiac myocyte function at different stages of PO-induced pathological LVH [8–10,22]. However, these studies share common limitations that warrants the need for further experimentations. First of all, most of the previous investigations analyzed myofilament function at only one specific time point (cross sectional studies). Consequently, we have limited data regarding the timeline of sarcomere changes in PO-induced LVH. Furthermore, none of the mentioned investigations assessed LV contractility in the same experimental model. Hence, our knowledge how the reported changes of myofilament function appear on global LV hemodynamics is also limited. Therefore, in the present investigation, we aimed to detect myofilament function and LV contractility from the same experimental animals at different stages of PO-induced LVH.

Early stage of PO-induced LVH. As we pointed it out above, the early stage of PO-induced LVH (AB-wk6 group) was associated with increased contractility (ESPVR, PRSW, dP/dt_{max}-EDV) on the global LV level. In the same experimental group, we observed enhanced Ca^{2+}-sensitivity (pCa_{50}) and unaltered F_{max} of permeabilized LV cardiomyocytes (Fig. 3 and Table 1). Therefore, our results indicate that increased myofilament Ca^{2+}-sensitivity held responsibility for the contractility augmentation on the cellular level during the early-phase of PO-induced LVH. Although, this kind of relation between myofilament Ca^{2+}-sensitivity and LV contractility in pathological LVH has not been postulated yet, numerous groups have reported increased sarcomere Ca^{2+}-sensitivity in pathological LVH with preserved systolic function [8,23]. Furthermore, to define the underlying molecular mechanism for the increased myofilament Ca^{2+}-sensitivity, we analyzed the phosphorylation status of specific regulatory sites of cTnI (Ser-23/24, Ser-43 and Thr-144) and cMyBP-C (Ser-282). These measurements revealed a robust increment in the phosphorylation of the PKC-dependent Thr-144 site of cTnI in the AB-wk6 group (Fig. 4C). In line with our results, it has been previously reported that pseudo-phosphorylation of cTnI at Thr-143/144 (Thr-143 in human and Thr-144 in mouse/rat) potentially enhances myofilament Ca^{2+}-sensitivity [24,25]. Interestingly, the hyperphosphorylation of Thr-143 site did not affect the maximal force development in human permeabilized cardiomyocytes [24], which finding is also in good agreement with our results demonstrating unaltered F_{max} in the AB-wk6 group (Table 1). Considering the fact that no alterations occurred at other sites of cTnI (Ser-22/23 and Ser-43) and cMyBP-C (Ser-282), it could be hypothesized that hyperphosphorylation of PKC-specific Thr-144 site of cTnI might have predominantly contributed to the increased myofilament Ca^{2+} sensitivity in the AB group at week 6.

Downloaded for Anonymous User (n/a) at HUNGARY - Debrecen University from ClinicalKey.com by Elsevier on March 22, 2019.
For personal use only. No other uses without permission. Copyright ©2019. Elsevier Inc. All rights reserved.

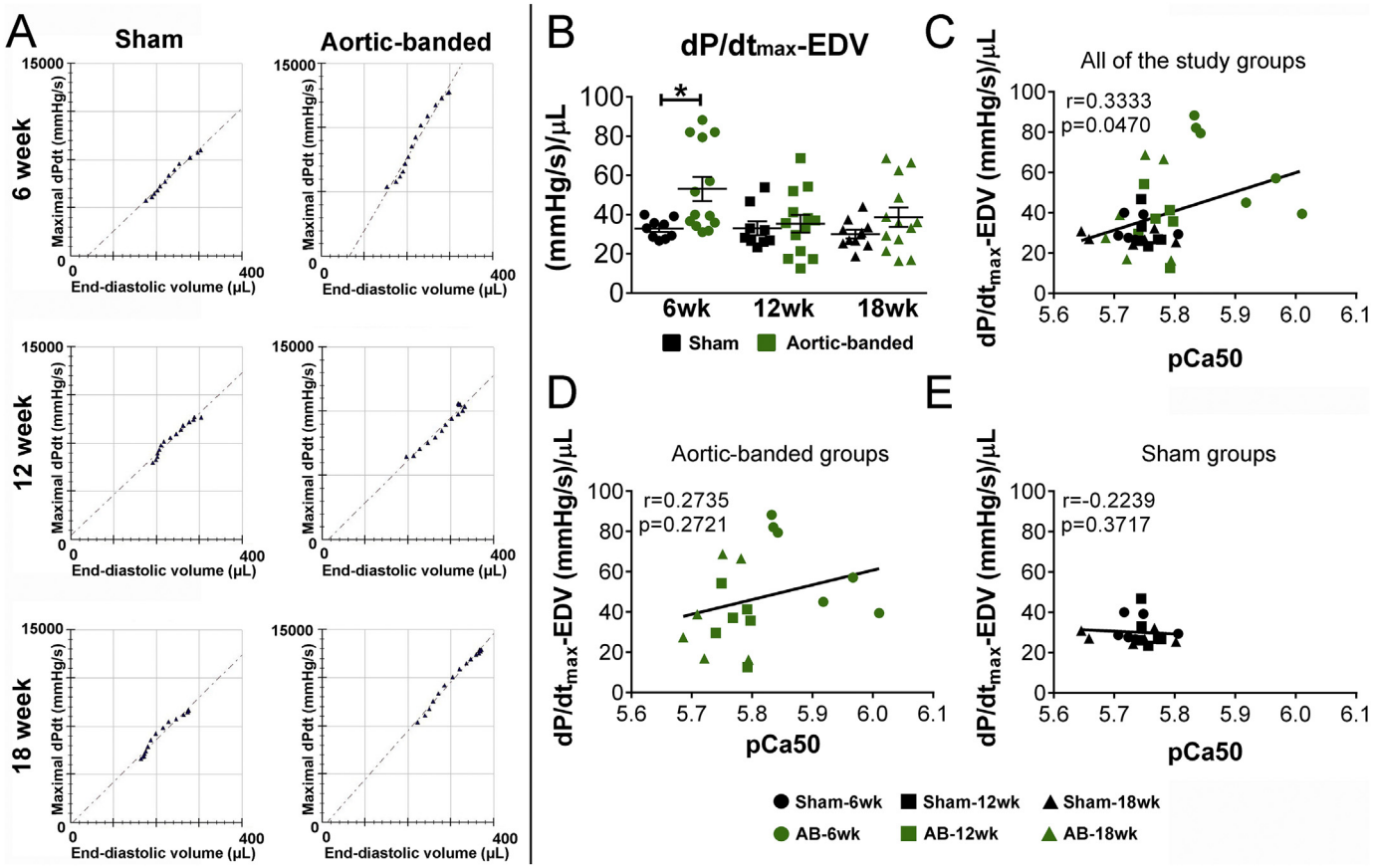

Fig. 7. Correlation between the maximal slope of the systolic pressure increment (dP/dt_{max})-end diastolic volume (EDV) relationship and myofilament Ca^{2+} sensitivity during the progression of pathological LVH.
Increment in dP/dt_{max}-EDV suggested increased left ventricular (LV) contractility in the aortic-banded (AB) group at week 6 compared to the corresponding sham group (A–B). Correlation was detected between in dP/dt_{max}-EDV and pCa_{50} among all the study groups (C). No correlation could be detected among only the AB (D) or the Sham groups (E). LVH indicates left ventricular hypertrophy. *: $P < .05$.

Advanced stages of PO-induced LVH. At more advanced stages of PO-induced LVH, the compensatory increment in LV contractility declined, as indicated by P—V analysis (Figs. 5B, 6B, 7B). In parallel, we found that the cellular (enhancement of myofilament Ca^{2+}-sensitivity) and molecular (cTnI hyperphosphorylation at PKC-specific Thr-144 site) adaptations also diminished in the AB groups at week 12 and 18 (Figs. 3, 4C). Therefore, in our longitudinal study, alterations of sarcomere Ca^{2+}-sensitivity as well as cTnI phosphorylation at Thr-144 followed very precisely the changes of LV contractility. Previous studies conducted on advanced stages of PO-induced LVH found normal or decreased Ca^{2+}-sensitivity in isolated and skinned single cardiomyocyte preparations. For instance, in a spontaneously hypertensive rat strain with evident signs of HF, neither pCa_{50} nor F_{max} differed from the control's level [22]. These results are in good agreement with the present findings, demonstrating the lack of cellular compensation to the increased PO in advanced stages of LVH. Furthermore, in a TAC-induced end-stage HF rat model, both components of myofilament function (pCa_{50}, F_{max}) were substantially decreased [9,10]. It is important to note that the aortic arch was constricted to a very severe level for a relatively long experimental period (36 weeks) in the latter studies. Therefore, it could be hypothesized that in this particular TAC model, the status of LVH and HF reached a more advanced level compared either to our abdominal AB or the spontaneously hypertensive rat models.

Based on our findings and the previous literature data, we hypothesize that increment in myofilament Ca^{2+}-sensitivity (due to hyperphosphorylation of the PKC-specific Thr-144 site of cTnI) represents an early but only temporary adaptation to increased PO. Accordingly, the initially increased sarcomere Ca^{2+}-sensitivity regresses during the transition from compensated LVH to early-stage HF and it substantially reduces at HF.

5. Conclusion

The present paper found that the early-stage of PO-induced LVH is associated with increased LV contractility on the intact organ level, and enhanced myofilament Ca^{2+} sensitivity (due to hyperphosphorylation of the PKC-specific Thr-144 site of cTnI) on the sarcomere level. This early functional adaption compensates for the increased afterload resulting in maintained ventriculo-arterial coupling and preserved systolic function. However, at more advanced stages of PO-induced LVH, the initial augmentation of LV contractility as well as the increased myofilament Ca^{2+} sensitivity decline, leading to impaired ventriculo-arterial coupling and reduced systolic performance. These data indicate, that changes in sarcomere Ca^{2+} sensitivity might underlie the alterations in LV contractility during the development and progression of PO-induced LVH.

Supplementary data to this article can be found online at https://doi.org/10.1016/j.yjmcc.2019.02.017.

Funding

The study was supported by the New National Excellence Program of the Ministry of Human Capacities (ÚNKP-18-3-I-SE-9; to M. Ruppert; ÚNKP-18-3-III-DE-387; to B. Bódi), the Higher Education Institutional Excellence Programme of the Ministry of Human Capacities in Hungary,

Downloaded for Anonymous User (n/a) at HUNGARY - Debrecen University from ClinicalKey.com by Elsevier on March 22, 2019.
For personal use only. No other uses without permission. Copyright ©2019. Elsevier Inc. All rights reserved.

within the framework of the Therapeutic Development thematic programme of the Semmelweis University, the National Research, Development and Innovation Office of Hungary (NKFIA; NVKP-16-1-2016-0017, 'National Heart Program'), the GINOP-2.3.2-15-2016-00048 project (the project is co-financed by the European Union and the European Regional Development Fund), the Land Baden-Württemberg, Germany, by the Medical Faculty of the University of Heidelberg, Germany (to S. Korkmaz-Icöz) and the János Bolyai Research Scholarship of the Hungarian Academy of Sciences (to T. Radovits). The research group of Zoltán Papp is supported by the Hungarian Academy of Sciences (11003).

Conflict of interest

None.

Acknowledgements

The excellent technical assistance of Patricia Kraft, Tobias Mayer, Karin Sonnenberg, Lutz Hoffmann, Henriett Biró, Edina Urbán, Alexandra Gephard and Erika Samodai is greatly acknowledged.

References

[1] B.P. Davidson, G.D. Giraud, Left ventricular function and the systemic arterial vasculature: remembering what we have learned, J. Am. Soc. Echocardiogr.Off. Publ. Am. Soc. Echocardiogr. 25 (2012) 891–894.
[2] P. Pacher, T. Nagayama, P. Mukhopadhyay, S. Batkai, D.A. Kass, Measurement of cardiac function using pressure–volume conductance catheter technique in mice and rats, Nat. Protoc. 3 (2008) 1422–1434.
[3] J. Chen, E.R. Chemaly, L.F. Liang, T.J. LaRocca, E. Yaniz-Galende, R.J. Hajjar, A new model of congestive heart failure in rats, Am. J. Physiol. Heart Circ. Physiol. 301 (2011) H994–1003.
[4] B.T. Nemeth, C. Matyas, A. Olah, A. Lux, L. Hidi, M. Ruppert, et al., Cinaciguat prevents the development of pathologic hypertrophy in a rat model of left ventricular pressure overload, Sci. Rep. 6 (2016) 37166.
[5] H.C. Ku, M.J. Su, DPP4 deficiency preserved cardiac function in abdominal aortic banding rats, PLoS One 9 (2014) e85634.
[6] M. Ruppert, S. Korkmaz-Icoz, S. Loganathan, W. Jiang, L.H. Lehmann, A. Olah, et al., Pressure–volume analysis reveals characteristic sex-related differences in cardiac function in a rat model of aortic banding-induced myocardial hypertrophy, Am. J. Physiol. Heart Circ. Physiol. 315 (2018) H502–H511.
[7] M. Ruppert, S. Korkmaz-Icoz, S. Li, B.T. Nemeth, P. Hegedus, P. Brlecic, et al., Myocardial reverse remodeling after pressure unloading is associated with maintained cardiac mechanoenergetics in a rat model of left ventricular hypertrophy, Am. J. Physiol. Heart Circ. Physiol. 311 (2016) H592–H603.
[8] N. Hamdani, K.G. Bishu, M. von Frieling-Salewsky, M.M. Redfield, W.A. Linke, Deranged myofilament phosphorylation and function in experimental heart failure with preserved ejection fraction, Cardiovasc. Res. 97 (2013) 464–471.
[9] R.J. Belin, M.P. Sumandea, T. Kobayashi, L.A. Walker, V.L. Rundell, D. Urboniene, et al., Left ventricular myofilament dysfunction in rat experimental hypertrophy and congestive heart failure, Am. J. Physiol. Heart Circ. Physiol. 291 (2006) H2344–H2353.
[10] R.J. Belin, M.P. Sumandea, G.A. Sievert, L.A. Harvey, D.L. Geenen, R.J. Solaro, et al., Interventricular differences in myofilament function in experimental congestive heart failure, Pflugers Archiv. Eur. J. Physiol. 462 (2011) 795–809.
[11] K. Sunagawa, W.L. Maughan, D. Burkhoff, K. Sagawa, Left ventricular interaction with arterial load studied in isolated canine ventricle, Am. J. Phys. 245 (1983) H773–H780.
[12] K. Yamamoto, The time constant of left ventricular relaxation: extrication from load dependence and overestimation of functional abnormality, Circ. Heart Fail. 3 (2010) 178–180.
[13] D.A. Kass, R. Beyar, E. Lankford, M. Heard, W.L. Maughan, K. Sagawa, Influence of contractile state on curvilinearity of in situ end-systolic pressure–volume relations, Circulation. 79 (1989) 167–178.
[14] D.A. Kass, R.P. Kelly, Ventriculo-arterial coupling: concepts, assumptions, and applications, Ann. Biomed. Eng. 20 (1992) 41–62.
[15] M. Ruppert, S. Korkmaz-Icoz, S. Li, B. Merkely, M. Karck, T. Radovits, et al., Reverse electrical remodeling following pressure unloading in a rat model of hypertension-induced left ventricular myocardial hypertrophy, Hyperten. Res. Off. J. Jpn. Soc. Hyperten. 40 (2017) 637–645.
[16] A. Olah, B.T. Nemeth, C. Matyas, L. Hidi, A. Lux, M. Ruppert, et al., Physiological and pathological left ventricular hypertrophy of comparable degree is associated with characteristic differences of in vivo hemodynamics, Am. J. Physiol. Heart Circ. Physiol. 310 (2016) H587–H597.
[17] J.R. McMullen, G.L. Jennings, Differences between pathological and physiological cardiac hypertrophy: novel therapeutic strategies to treat heart failure, Clin. Exp. Pharmacol. Physiol. 34 (2007) 255–262.
[18] S.E. Litwin, S.E. Katz, E.O. Weinberg, B.H. Lorell, G.P. Aurigemma, P.S. Douglas, Serial echocardiographic-Doppler assessment of left ventricular geometry and function in rats with pressure-overload hypertrophy. Chronic angiotensin-converting enzyme inhibition attenuates the transition to heart failure, Circulation. 91 (1995) 2642–2654.
[19] P.S. Douglas, B. Berko, M. Lesh, N. Reichek, Alterations in diastolic function in response to progressive left ventricular hypertrophy, J. Am. Coll. Cardiol. 13 (1989) 461–467.
[20] A.C. Gomes, I. Falcao-Pires, A.L. Pires, C. Bras-Silva, A.F. Leite-Moreira, Rodent models of heart failure: an updated review, Heart Fail. Rev. 18 (2013) 219–249.
[21] N. Hamdani, V. Kooij, S. van Dijk, D. Merkus, W.J. Paulus, C.D. Remedios, et al., Sarcomeric dysfunction in heart failure, Cardiovasc. Res. 77 (2008) 649–658.
[22] C.L. Perreault, O.H. Bing, W.W. Brooks, B.J. Ransil, J.P. Morgan, Differential effects of cardiac hypertrophy and failure on right versus left ventricular calcium activation, Circ. Res. 67 (1990) 707–712.
[23] B. Fraysse, F. Weinberger, S.C. Bardswell, F. Cuello, N. Vignier, B. Geertz, et al., Increased myofilament Ca2+ sensitivity and diastolic dysfunction as early consequences of Mybpc3 mutation in heterozygous knock-in mice, J. Mol. Cell. Cardiol. 52 (2012) 1299–1307.
[24] P.J. Wijnker, V. Sequeira, D.B. Foster, Y. Li, C.G. Dos Remedios, A.M. Murphy, et al., Length-dependent activation is modulated by cardiac troponin I bisphosphorylation at Ser23 and Ser24 but not by Thr143 phosphorylation, Am. J. Physiol. Heart Circ. Physiol. 306 (2014) H1171–H1181.
[25] H. Wang, J.E. Grant, C.M. Doede, S. Sadayappan, J. Robbins, J.W. Walker, PKC-betaII sensitizes cardiac myofilaments to Ca2+ by phosphorylating troponin I on threonine-144, J. Mol. Cell. Cardiol. 41 (2006) 823–833.

Downloaded for Anonymous User (n/a) at HUNGARY - Debrecen University from ClinicalKey.com by Elsevier on March 22, 2019.
For personal use only. No other uses without permission. Copyright ©2019. Elsevier Inc. All rights reserved.